

Probing the Factors That Stabilize Mononuclear Rhodium(II) Bis(phosphine), η^6 -Arene Complexes with Piano-Stool Geometries

Elizabeth T. Singewald,[†] Caroline S. Slone,[†] Charlotte L. Stern,[†]
Chad A. Mirkin,^{*,†} Glenn P. A. Yap,[‡] Louise M. Liable-Sands,[‡] and
Arnold L. Rheingold[‡]

Contribution from the Department of Chemistry, Northwestern University, Evanston, Illinois 60208-3113, and Department of Chemistry and Biochemistry, University of Delaware, Newark, Delaware 19716

Received September 26, 1996. Revised Manuscript Received January 2, 1997[⊗]

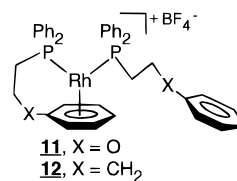
Abstract: The synthesis, characterization, and electrochemistry of a series of Rh(I) bis(phosphine), η^6 -arene, piano-stool complexes are reported. The study reported herein elucidates several of the important factors which lead to the stabilization of Rh(II) in this coordination environment. From the electrochemical data for a series of complexes of the type $[\text{Rh}(\eta^2\text{-dippe})(\eta^6\text{-C}_6\text{H}_{6-n}\text{X}_n)]\text{BF}_4$ ($\text{X} = \text{CH}_3$, $n = 0\text{--}6$) (**1–7**) it was shown that the addition of methyl groups to the arene ligand kinetically stabilize the Rh(II) center and thermodynamically stabilize the Rh(II) species by 16 mV per added methyl group. Furthermore, complexes which contain chelation to the arene ligand, such as $[\text{Rh}(\eta^6:\eta^1\text{-Ph}(\text{CH}_2)_3\text{PPh}_2)(\eta^1\text{-Ph}(\text{CH}_2)_3\text{PPh}_2)]\text{BF}_4$ (**12**), kinetically stabilize the Rh(II) form, presumably from ligand substitution based decomposition reactions. The electrochemical studies of five isostructural and isoelectronic complexes, $[\text{Rh}(\eta^2\text{-dippe})(\eta^6\text{-C}_6\text{H}_5\text{CH}_3)]\text{BF}_4$ (**2**), $[\text{Rh}(\eta^1\text{-}n\text{-BuPPH}_2)_2(\eta^6\text{-C}_6\text{H}_5\text{CH}_3)]\text{BF}_4$ (**8**), $[\text{Rh}(\eta^2\text{-dppp})(\eta^6\text{-C}_6\text{H}_5\text{-CH}_3)]\text{BF}_4$ (**9**), $[\text{Rh}(\eta^2\text{-dppb})(\eta^6\text{-C}_6\text{H}_5\text{CH}_3)]\text{BF}_4$ (**10**), and **12** show that those complexes which contain bidentate, bis(phosphine) chelation with an ethyl or butyl bridge, **2** and **10**, thermodynamically destabilize the Rh(II) form relative to those complexes which contain a less restricted bis(phosphine) chelate or no bis(phosphine) chelation. Using single-crystal X-ray data and extended Hückel calculations, these counterintuitive electrochemical trends were explained in terms of not only the properties of the Rh(I) complex but also, in terms of the structural changes which are likely to occur upon oxidation of the metal center from Rh(I) to Rh(II).

Introduction

Rh(I) and Rh(III) complexes are known to play an enormous role in the mechanistic cycles of many catalytic processes,¹ and therefore, it is not surprising that Rh complexes in these oxidation states have been studied extensively. In comparison, little is known about the chemistry of Rh(II) complexes,² especially monomeric, *organometallic* Rh(II) compounds.³ Of the isolable compounds known, all adopt either square-planar or sandwich coordination geometries.

In recent years, our group has been engaged in the development of the chemistry of Rh(I) bis(alkylphosphine), η^6 -arene

Chart 1



complexes, **11** and **12**⁴ (Chart 1). The general class of cationic Rh(I) η^6 -arene, piano-stool complexes, without tethered arene ligands, has been studied by various research groups since the early 1970s.⁵ Our complexes, in addition to exhibiting unusual dynamic intramolecular arene exchange behavior^{4a–c} and catalytic processes that can be controlled with redox-active arene substituents,^{4d} exhibit reversible electrochemistry associated with their Rh(I)/(II) redox couples.^{4a–c} From such preliminary experiments, we concluded that these complexes support Rh(II) oxidation states that are stable at least on the time scale of the electrochemical experiments performed. Therefore, such studies suggest that modification of the ligands, perhaps even minor ones, may give entry into a new class of isolable, Rh(II) compounds.

Herein, we report the synthesis, characterization, and electrochemical properties for a series of isostructural and isoelectronic Rh(I) complexes **1–10** (Chart 2). In addition, the single-crystal X-ray diffraction and extended Hückel studies of **5**, **8**,

[†] Northwestern University

[‡] University of Delaware.

* Author to whom correspondence should be addressed.

⊗ Abstract published in *Advance ACS Abstracts*, March 15, 1997.

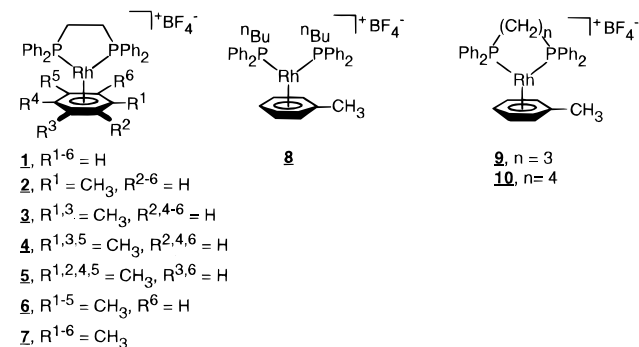
(1) (a) Parshall, G. W.; Ittel, S. D. *Homogeneous Catalysis*; Wiley-Interscience: New York, 1992. (b) Dickson, R. S. *Homogeneous Catalysis with Compounds of Rhodium and Iridium*; D. Reidel Publishing Co.: Dordrecht, Holland, 1985. (c) Collman, J. P.; Hegedus, L. S.; Norton, J. R.; Finke, R. G. *Principles and Applications of Organotransition Metal Chemistry*; University Science Books: Mill Valley, CA, 1987.

(2) Rh(II) reactivity studies: (a) Howe, J. P.; Lung, K.; Nile, T. A. *J. Organomet. Chem.* **1981**, 208, 401. (b) Arzoumanian, H.; Blanc, A. A.; Metzger, J.; Vincent, J. E. *J. Organomet. Chem.* **1974**, 82, 261. Dimeric Rh(II): (c) Cotton, F. A.; Walton, R. A. *Multiple Bonds Between Metal Atoms*; Wiley Interscience: New York, 1982, p 311. Rh(II) reviews: (d) Pandey, K. K. *Coord. Chem. Rev.* **1992**, 121, 1. (e) DeWit, D. G. *Coord. Chem. Rev.* **1996**, 147, 209.

(3) (a) Collins, J. E.; Castellani, M. P.; Rheingold, A. L.; Miller, E. J.; Geiger, W. E.; Rieger, A. L.; Rieger, P. H. *Organometallics* **1995**, 14, 1232. (b) García, M. P.; Jiménez, M. V.; Oro, L. A.; Lahoz, F. J.; Casas, J. M.; Alonso, P. J. *Organometallics* **1993**, 12, 3257. (c) Dunbar, K. R.; Haefner, S. C. *Organometallics* **1992**, 11, 1431. (d) Hay-Motherwell, R. S.; Koschmieder, S. U.; Wilkinson, G.; Hussain-Bates, B.; Hursthouse, M. B. *J. Chem. Soc., Dalton Trans.* **1991**, 2821. (e) Bowyer, W. J.; Merkert, J. W.; Geiger, W. E.; Rheingold, A. L. *Organometallics* **1989**, 8, 191.

(4) (a) Singewald, E. T.; Mirkin, C. A.; Levy, A. D.; Stern, C. L. *Angew. Chem., Int. Ed. Engl.* **1994**, 33, 2473; *Angew. Chem.* **1994**, 106, 2524. (b) Singewald, E. T.; Shi, X.; Mirkin, C. A.; Schofer, S. J.; Stern, C. L. *Organometallics* **1996**, 15, 3062. (c) Sassano, C. A.; Mirkin, C. A. *J. Am. Chem. Soc.* **1995**, 117, 11379. (d) Slone, C. S.; Mirkin, C. A. Unpublished results.

Chart 2



9, and **12** are presented. These piano-stool compounds allow for the systematic determination of the fundamental factors that control the stability of Rh(II) in complexes with this coordination geometry. Such factors include (1) the arene substituents, (2) the presence (**1–7**, **9**, **10**, or **12**) or absence (**8**) of ligand chelation, (3) the type of ligand chelation (by a bis(phosphine) ligand as in **1** or through a (phosphinoalkyl)arene ligand as in **12**), and (4) the structural changes which may occur on oxidation of the metal center. To the best of our knowledge, this is the most extensive systematic electrochemical, structural, and spectroscopic study of a set of isoelectronic Rh(I) complexes yet reported and, significantly, it elucidates several *counterintuitive* factors that control the electron richness and stabilities of the Rh(II) centers in this coordination geometry that should extend well beyond this important class of compounds.

Experimental Section

General Procedure. All reactions were carried out under nitrogen using standard Schlenk techniques or in an inert atmosphere glovebox. Methylene chloride was distilled from calcium hydride. Tetrahydrofuran (THF) was dried over sodium/benzophenone. Benzene, toluene, and 1,3,5-trimethylbenzene were dried over sodium. Methanol was dried over MgO. All solvents were distilled and degassed prior to use. Deuterated solvents were purchased in ampules from Cambridge Isotope Laboratories and used without further purification. *n*-Butyldiphenylphosphine was purchased from Lancaster Chemical Co. and distilled over sodium prior to use. RhCl₃·xH₂O was used on loan from Johnson-Matthey Chemical Co. Compounds **1** and **2** were prepared according to the method of Halpern.^{5c,d} Compound **12**,^{4a,b} [Rh(μ -Cl)(η^2 -C₈H₁₄)₂]₆,⁶ [Rh(η^4 -C₇H₈)(η^2 -dppe)]BF₄ (dppe = 1,2-bis(diphenylphosphino)ethane),⁷ and [Rh(η^4 -C₇H₈)(η^2 -dppp)]BF₄ (dppp = 1,3-bis(diphenylphosphino)propane)⁷ were prepared according to literature procedures. All other chemicals were purchased from Aldrich Chemical Co. and used as received.

Physical Measurements. ¹H and ¹³C{¹H} NMR spectra were recorded on either a Varian Gemini 300 MHz, a Varian VXR 300 MHz, or a Varian Unity 400 MHz FT-NMR spectrometer. ³¹P{¹H} NMR spectra were recorded on a Varian Gemini 300 MHz FT-NMR spectrometer at 121 Hz and referenced versus the external standard 85% H₃PO₄. Electrochemical measurements were carried out on either a PINE AFRDE4 or AFRDE5 bipotentiostat (CV) or a PAR 273A potentiostat/galvanostat (DPV) using a Pt working electrode (0.02 cm²), a Pt mesh counter electrode, and a Ag wire reference electrode. Rotating disk voltammetry experiments were carried out using a PINE Pt rotating disk electrode at 1000 rotations/min. In all cases, a 0.1 M

solution of *n*-Bu₄NPF₆ in CH₂Cl₂ was used as the supporting electrolyte. All electrochemical data are referenced versus the FcH/[FcH]⁺ [Fc = (η^5 -C₅H₅)Fe(η^5 -C₅H₄)] redox couple. Fast atom bombardment (FAB) mass spectra were recorded on a Fisons VG 70-250 SE mass spectrometer. High-resolution mass spectrometry data were not attainable for many of the compounds reported due to low intensity of the parent peaks in the spectra relative to the baseline noise.

[Rh(η^6 -benzene)(η^2 -dppe)]tetrafluoroborate (1**).** ¹H NMR (CD₂Cl₂): δ 2.25 (d, 4H, *J*_{P-H} = 21.3 Hz, CH₂), 6.31 (s, 6H, C₆H₆), 7.53 (m, 20H, P(C₆H₅)₂). ¹³C{¹H} NMR (CD₂Cl₂): δ 25.53 (m, CH₂), 101.94 (s, C₆H₆), 128.63–132.51 (m, P(C₆H₅)₂). FABMS: [M⁺] = *m/z* 579.

[Rh(η^6 -toluene)(η^2 -dppe)]tetrafluoroborate (2**).** ¹H NMR (CD₂Cl₂): δ 1.68 (s, 3H, CH₃), 2.24 (d, 4H, *J*_{P-H} = 21.4 Hz, CH₂), 6.17 (m, 2H, *o*-C₆H₅CH₃), 6.30 (m, 2H, *m*-C₆H₅CH₃), 7.20 (m, 1H, *p*-C₆H₅-CH₃), 7.55 (m, 20H, P(C₆H₅)₂). ¹³C{¹H} NMR (CD₂Cl₂): δ 19.37 (s, CH₃), 29.87 (m, CH₂), 100.89 (s, C₆H₅CH₃), 103.04 (s, C₆H₅CH₃), 118.34 (s, C₆H₅CH₃), 125.55 (s, C₆H₅CH₃), 128.48–132.61 (m, P(C₆H₅)₂). FABMS: [M⁺] = *m/z* 593.

Synthesis of [Rh(η^6 -1,3-dimethylbenzene)(η^2 -dppe)]tetrafluoroborate (3**).** [Rh(η^4 -C₇H₈)(η^2 -dppe)]BF₄ (40 mg, 0.06 mmol) in 5 mL of CH₃OH was bubbled with H₂ for 5 min. The color of the solution gradually changed from orange to yellow. The solution was concentrated to 3 mL, and 25 mL of 1,3-dimethylbenzene (5 equiv, 0.20 mol) was added. After 12 h of stirring at room temperature, the solvent was removed. Pure product **3** was isolated in quantitative yield based on spectroscopic data (yield = 40 mg, 0.06 mmol, >99%). ¹H NMR (CD₂Cl₂): δ 1.74 (s, 6H, CH₃), 2.19 (d, 4H, *J*_{P-H} = 21.6 Hz, CH₂), 6.00 (m, 3H, *o*, *p*-C₆H₄(CH₃)₂), 6.26 (t, 1H, *J*_{H-H} = 6.8 Hz, *m*-C₆H₄(CH₃)₂), 7.55 (m, 20H, P(C₆H₅)₂). ¹³C{¹H} NMR (CD₂Cl₂): δ 19.47 (s, CH₃), 30.20 (m, CH₂), 100.33 (s, C₆H₄(CH₃)₂), 101.57 (s, C₆H₄(CH₃)₂), 105.13 (s, C₆H₄(CH₃)₂), 116.99 (s, C₆H₄(CH₃)₂), 128.29–133.98 (m, P(C₆H₅)₂). HRFABMS: [M⁺] calcd = *m/z* 607.1191, [M⁺] found = *m/z* 607.1187.

Synthesis of [Rh(η^6 -1,3,5-trimethylbenzene)(η^2 -dppe)]tetrafluoroborate (4**).** Synthesis of **4** is identical to the synthesis of **3** except 1,3,5-trimethylbenzene is used as the arene (yield = >95%). ¹H NMR (CD₂Cl₂): δ 1.79 (s, 9H, CH₃), 2.16 (d, 4H, *J*_{P-H} = 21.0 Hz, CH₂), 5.85 (s, 3H, C₆H₃(CH₃)₃), 7.56 (m, 20H, P(C₆H₅)₂). ¹³C{¹H} NMR (CD₂Cl₂): δ 19.75 (s, CH₃), 31.74 (m, CH₂), 103.53 (s, C₆H₃(CH₃)₃), 116.25 (s, C₆H₃(CH₃)₃), 129.34–133.88 (m, P(C₆H₅)₂). FABMS: [M⁺] = *m/z* 621.

Synthesis of [Rh(η^6 -1,2,4,5-tetramethylbenzene)(η^2 -dppe)]tetrafluoroborate (5**).** Synthesis of **5** is identical to the synthesis of **3** except 2,4,5-tetramethylbenzene was used as the arene. Complex **5** is purified by washing away excess 1,2,4,5-tetramethylbenzene with three 5 mL portions of benzene and removing any excess solvent by vacuum evaporation (yield = >95%). ¹H NMR (CD₂Cl₂): δ 1.69 (s, 12H, CH₃), 2.12 (d, 4H, *J*_{P-H} = 21.5 Hz, CH₂), 5.80 (s, 2H, C₆H₂(CH₃)₄), 7.57 (m, 20H, P(C₆H₅)₂). ¹³C{¹H} NMR (CD₂Cl₂): δ 17.44 (s, CH₃), 30.02 (m, CH₂), 102.72 (s, C₆H₂(CH₃)₄), 116.08 (s, C₆H₂(CH₃)₄), 129.34–133.30 (m, P(C₆H₅)₂). HRFABMS: [M⁺] calcd = *m/z* 635.1504, [M⁺] found = *m/z* 635.1486.

Synthesis of [Rh(η^6 -pentamethylbenzene)(η^2 -dppe)]tetrafluoroborate (6**).** Synthesis of **6** is identical to the synthesis of **5** except 1,2,3,4,5-pentamethylbenzene is used as the arene (yield = >95%). ¹H NMR (CD₂Cl₂): δ 1.68 (s, 6H, CH₃), 1.72 (s, 6H, CH₃), 1.80 (s, 3H, CH₃), 2.04 (d, 4H, *J*_{P-H} = 21.6 Hz, CH₂), 5.78 (s, 1H, C₆H(CH₃)₅), 7.57 (m, 20H, P(C₆H₅)₂). ¹³C{¹H} NMR (CD₂Cl₂): δ 14.11 (s, CH₃), 15.26 (s, CH₃), 18.08 (s, CH₃), 29.99 (m, CH₂), 101.68 (s, C₆H(CH₃)₅), 112.73 (s, C₆H(CH₃)₅), 113.68 (s, C₆H(CH₃)₅), 114.48 (s, C₆H(CH₃)₅), 128.42–132.13 (m, P(C₆H₅)₂). HRFABMS: [M⁺] calcd = *m/z* 649.1660, [M⁺] found = *m/z* 649.1646.

Synthesis of [Rh(η^6 -hexamethylbenzene)(η^2 -dppe)]tetrafluoroborate (7**).** Synthesis of **7** is identical to the synthesis of **5** except 1,2,3,4,5,6-hexamethylbenzene is used as the arene (yield = >95%). ¹H NMR (CD₂Cl₂): δ 1.75 (s, 18H, CH₃), 1.95 (d, 4H, *J*_{P-H} = 21.0 Hz, CH₂), 7.59 (m, 20H, P(C₆H₅)₂). ¹³C{¹H} NMR (CD₂Cl₂): δ 16.27 (s, CH₃), 30.73 (m, CH₂), 113.52 (s, C₆(CH₃)₆), 129.33–133.23 (m, P(C₆H₅)₂); HRFABMS: [M⁺] calcd = *m/z* 663.1817, [M⁺] found = *m/z* 663.1837.

(5) (a) Schrock, R. R.; Osborn, J. A. *J. Am. Chem. Soc.* **1971**, *93*, 3089. (b) Green, M.; Kuc, T. A. *J. Chem. Soc., Dalton Trans.* **1972**, 832. (c) Halpern, J.; Riley, D. P.; Chan, A. S. C.; Pluth, J. J. *J. Am. Chem. Soc.* **1977**, *99*, 8055. (d) Halpern, J.; Chan, A. S. C.; Riley, D. P.; Pluth, J. J. *Adv. Chem. Ser.* **1979**, No. 173, 16. (e) Uson, R.; Lahuerta, P.; Reyes, J.; Oro, L. A.; Foces-Foces, C.; Cano, F. H.; Garcia-Blanco, S. *Inorg. Chim. Acta* **1980**, *42*, 832.

(6) Porri, L.; Lionetti, A.; Immirizi, A. *Chem. Commun.* **1965**, 356. (7) Brown, J. M.; Chaloner, P. A.; Kent, A. G.; Murrer, B. A.; Nicholson, P. N.; Parker, D.; Sidebottom, P. J. *J. Organomet. Chem.* **1981**, *216*, 263.

Table 1. Crystallographic Data for **5**, **8**, and **12**

	5	8	12
formula	C ₃₆ H ₃₈ BF ₄ P ₂ Rh	C ₃₉ H ₄₆ BF ₄ P ₂ Rh	C ₄₂ H ₄₂ BF ₄ P ₂ Rh
fw	722.32	766.42	798.45
crystal system	monoclinic	orthorhombic	monoclinic
space group	<i>P</i> 2 ₁ / <i>c</i>	<i>Pca</i> 2 ₁	<i>Cc</i>
<i>a</i> , Å	15061(2)	13.341(3)	16.828(3)
<i>b</i> , Å	11.308(1)	19.017(3)	12.039(4)
<i>c</i> , Å	19.880(1)	18.264(4)	19.092(6)
β, deg	102.741(6)		107.78(2)
<i>V</i> , Å ³	3302.4(6)	3592(2)	3683(3)
<i>Z</i>	4	4	4
<i>D</i> _{calc} , g cm ⁻³	1.453	1.417	1.440
color	orange	orange	orange
size, mm	0.40 × 0.40 × 0.30	0.40 × 0.20 × 0.05	0.22 × 0.51 × 0.14
μ (Mo Kα), cm ⁻¹	6.61	6.13	5.90
temp, K	298	247	153
radiation	Mo Kα	Mo Kα	Mo Kα
<i>R</i> (<i>F</i>), %	3.68	4.19	2.7
<i>R</i> (<i>wF</i>), %	8.08	7.33	3.2

Synthesis of [Rh(η⁶-toluene)(CH₃(CH₂)₃P(C₆H₅)₂)₂]tetrafluoroborate (8**).** Compound **8** was synthesized by reacting [Rh(μ-Cl)(η²-C₈H₁₄)₂]_x (0.078 g, 0.22 mmol) with 2 equiv of *n*-BuP(C₆H₅)₂ (0.11 g, 0.44 mmol, 0.10 mL) in THF (5 mL) at room temperature under constant stirring. After 30 min, 1 equivalent of AgBF₄ (0.042 g, 0.22 mmol) and excess toluene (2 mL) were added to the solution while the reaction mixture was continually stirred. After 1 h, the reaction mixture was filtered to remove AgCl and evaporated to dryness. The product **8** was isolated as a microcrystalline orange solid (0.147 g, 0.21 mmol, yield = 95%). ¹H NMR (CD₂Cl₂): δ 0.79 (t, 3H, *J*_{H-H} = 7.2 Hz, CH₂CH₃), 1.21 (m, 2H, CH₂CH₃), 1.36 (m, 2H, PCH₂CH₂CH₂), 1.70 (m, 2H, PCH₂), 2.25 (s, 3H, C₆H₅CH₃), 5.61 (d, 2H, *J*_{H-H} = 6.6 Hz, *o*-C₆H₅CH₃), 5.71 (t, 2H, *J*_{H-H} = 6.6 Hz, *m*-C₆H₅CH₃), 6.87 (t, 1H, *J*_{H-H} = 6.3 Hz, *p*-C₆H₅-CH₃), 7.19 and 7.38 (m, 20H, P(C₆H₅)₂). FABMS: [M⁺] = *m/z* 679.

Synthesis of [Rh(η⁶-toluene)(η²-dppp)]tetrafluoroborate (9**).** [Rh(η⁴-C₇H₈)(η²-dppp)]BF₄ (20 mg, 0.03 mmol) was dissolved in methanol-*d*₄ (0.5 mL) in an NMR tube, and the tube was charged with H₂. After 10 h, the diene was completely hydrogenated to form [Rh(CD₃OD)₂(η²-dppp)]BF₄ and excess toluene (1 mL) was added to the NMR tube. After 2 h, the formation of product **9** was complete in quantitative spectroscopic yield. ¹H NMR (CD₂Cl₂): δ 1.87 (m, 2H, PCH₂CH₂), 1.91 (s, 3H, CH₃), 2.48 (m, 4H, PCH₂), 5.66 (d, 2H, *J*_{H-H} = 6.3 Hz, *o*-C₆H₅CH₃), 5.80 (t, 2H, *J*_{H-H} = 6.7 Hz, *m*-C₆H₅CH₃), 6.15 (t, 1H, *J*_{H-H} = 6.3 Hz, *p*-C₆H₅CH₃), 7.45 (m, 20H, P(C₆H₅)₂). FABMS: [M⁺] = *m/z* 607.

Synthesis of [Rh(η⁶-toluene)(η²-dppb)]tetrafluoroborate (10**).** Complex **10** was synthesized in a manner similar to the synthesis of **9**, except [Rh(η⁴-C₈H₁₂)(η²-dppb)]BF₄ was used as the starting material (spectroscopic yield = >99%). ¹H NMR (CD₂Cl₂): δ 1.56 (m, 4H, PCH₂CH₂), 1.95 (s, 3H, CH₃), 2.39 (m, 4H, PCH₂), 5.32 (d, 2H, *J*_{H-H} = 6.5 Hz, *o*-C₆H₅CH₃), 5.45 (t, 2H, *J*_{H-H} = 6.6 Hz, *m*-C₆H₅CH₃), 6.62 (t, 1H, *J*_{H-H} = 6.3 Hz, *p*-C₆H₅CH₃), 7.56 (m, 20H, P(C₆H₅)₂). HRFABMS: [M⁺] calcd = *m/z* 621.1347, [M⁺] found = *m/z* 621.1359.

X-ray Structure Determinations. Crystals of **5** suitable for X-ray diffraction were grown in a methylene chloride solution by slow evaporation. Selected crystallographic data are given in Table 1. The systematic absences in the diffraction data are uniquely consistent for the reported space group, *P*2₁/*c*. The structure was solved using direct methods, completed by subsequent difference Fourier syntheses, and refined by full-matrix least-squares procedures. Absorption corrections were not applied because there was less than 10% variation in the ψ-scan data. All non-hydrogen atoms were refined with anisotropic displacement coefficients. Hydrogen atoms were treated as idealized contributions.^{8a}

(8) All software and sources of the scattering factors are contained in the (a) SHELXTL (5.3) program library or (b) SHELXS-86 (G. Sheldrick, Siemens XRD, Madison, WI). (c) Selected crystallographic data for **9**: crystal system = monoclinic; space group = *Pnma*; unit cell parameters = *a* (17.109(6) Å), *b* (20.858(9) Å), *c* (11.083(4) Å), *V* (3955(3) Å³); Rh-P = 2.223(2) Å; P-Rh-P = 91.74(11)°

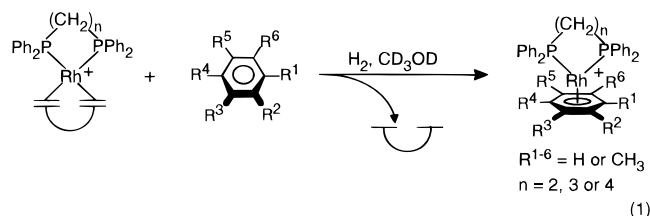
Crystals of **8** were grown from a 1:10 mixture of THF and toluene. Selected crystallographic data are given in Table 1. The unit-cell parameters were obtained by the least-squares refinement of the angular settings of 24 reflections (20° ≤ 2θ ≤ 24°). The systematic absences in the diffraction data are consistent with the space groups *Pcam* (*Pbcm*) and *Pca*2₁. Both options were explored; however, the centrosymmetric space group yielded chemically bizarre and computationally unstable results. The structure was solved in *Pca*2₁ using direct methods, completed by subsequent difference Fourier syntheses, and refined by full-matrix least-squares procedures. Refinement of the Flack parameter suggested racemic twinning and the structure was subsequently refined with scale factors as a 70/30 racemate. A semiempirical absorption correction was applied to the data set. The phenyl rings were treated as rigid groups. All non-hydrogen atoms were refined with anisotropic displacement coefficients. Hydrogen atoms were treated as idealized contributions.^{8a}

Crystals of **9** were grown from a 1:1 mixture of methanol-*d*₄ and toluene.^{8c} All inspected crystals were either twinned or multiple and complicated single-crystal X-ray diffraction studies. A low-quality structure was determined (see Supporting Information) and is referred to here in terms of connectivity and, specifically, the P-Rh-P bond angle (91.74° (11)) and Rh-P bond length (2.223 (2) Å).

Complex **12** was synthesized according to literature methods and crystals suitable for diffraction were grown from a 1:10 mixture of methylene chloride and diethyl ether.^{4a,b} Selected crystallographic data are given in Table 1. The systematic absences are consistent for the space groups *Cc* and *C2/c*. On the basis of packing considerations, a statistical analysis of the intensity distribution, and the successful refinement of the structure, the space group was determined to be *Cc*. The structure was solved by Patterson methods.^{8b} The data were corrected for Lorentz and polarization effects. In addition, an analytical absorption correction was applied with transmission factors ranging from 0.80 to 0.91, and a correction for secondary extinction was applied (coefficient = 0.21105 × 10⁻⁷). All hydrogen atoms were treated as idealized contributions.^{8b}

Results and Discussion

Syntheses of 1–10. Complexes **1–7**, **9**, and **10** were synthesized by reacting the appropriate [Rh(η⁴-diene)(η²-bis(phosphine))]BF₄ precursor with hydrogen in the presence of CD₃OD or CH₃OH and subsequently adding an excess amount of the appropriate arene ligand, eq 1. Complex **8** was



synthesized by reacting 1 equiv of [Rh(μ-Cl)(η²-C₈H₁₄)₂]₆ with 2 equiv of *n*-BuPPh₂, followed by halide abstraction with AgBF₄ in the presence of excess toluene. All complexes were isolated in high yield (> 95%). The benzene and the toluene adducts, **1** and **2**, respectively, were originally synthesized by Halpern and co-workers.^{5c,d} Complexes **3–10** are new and have been fully characterized (see the Experimental Section).

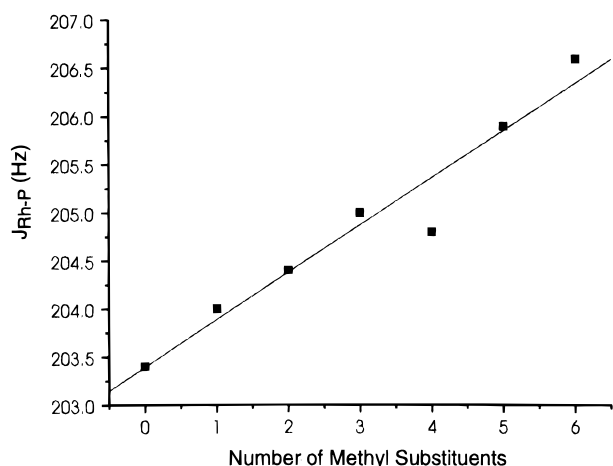
Selected ¹H, ¹³C, and ³¹P NMR Data for 1–10. Complexes **1–10** exhibit characteristic upfield shifts for the ¹H and ¹³C NMR resonances assigned to the η⁶-arenes. In the ¹H NMR spectra of **1–10**, the η⁶-arene resonances shift an average of 1.0 ppm upfield upon coordination to the metal in all complexes. Upfield shifts also are observed in the ¹³C NMR spectra for **1–7** of 17.8–28.5 ppm, depending on the arene.⁹ Such ¹H and ¹³C NMR upfield shifts are characteristic for arenes coordinated in an η⁶-fashion to a metal center.¹⁰

(9) Compounds **8–10** were not characterized by ¹³C NMR spectroscopy.

Table 2. Electrochemical^a and ³¹P NMR^b Data for Complexes **1–12**

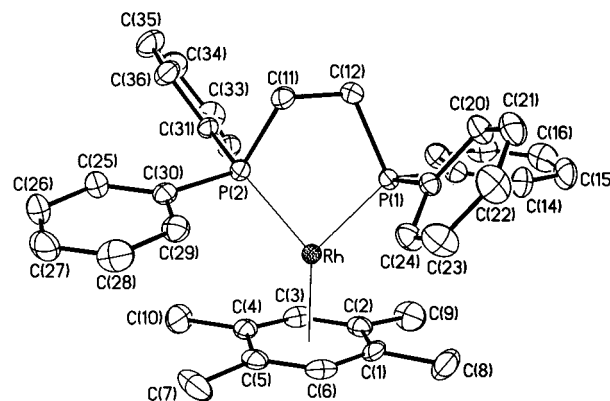
complex	$E_{1/2}$ (mV)	δ	$J_{\text{Rh-P}}$ (Hz)
1 [Rh(η^6 -C ₆ H ₆)(η^2 -(C ₆ H ₅) ₂ P(CH ₂) ₂ P(C ₆ H ₅) ₂)]BF ₄	irreversible	77.3	203.4
2 [Rh(η^6 -C ₆ H ₅ CH ₃)(η^2 -(C ₆ H ₅) ₂ P(CH ₂) ₂ P(C ₆ H ₅) ₂)]BF ₄	635	78.1	204.0
3 [Rh(η^6 -C ₆ H ₄ (CH ₃) ₂)(η^2 -(C ₆ H ₅) ₂ P(CH ₂) ₂ P(C ₆ H ₅) ₂)]BF ₄	620	78.7	204.4
4 [Rh(η^6 -C ₆ H ₃ (CH ₃) ₃)(η^2 -(C ₆ H ₅) ₂ P(CH ₂) ₂ P(C ₆ H ₅) ₂)]BF ₄	609	79.4	205.0
5 [Rh(η^6 -C ₆ H ₂ (CH ₃) ₄)(η^2 -(C ₆ H ₅) ₂ P(CH ₂) ₂ P(C ₆ H ₅) ₂)]BF ₄	590	79.6	204.8
6 [Rh(η^6 -C ₆ H(CH ₃) ₅)(η^2 -(C ₆ H ₅) ₂ P(CH ₂) ₂ P(C ₆ H ₅) ₂)]BF ₄	571	79.3	205.9
7 [Rh(η^6 -C ₆ (CH ₃) ₆)(η^2 -(C ₆ H ₅) ₂ P(CH ₂) ₂ P(C ₆ H ₅) ₂)]BF ₄	555	79.5	206.6
8 [Rh(η^6 -C ₆ H ₅ CH ₃)(η^1 - <i>n</i> -BuPPh ₂) ₂]]BF ₄	505	35.3	202.3
9 [Rh(η^6 -C ₆ H ₅ CH ₃)(η^2 -(C ₆ H ₅) ₂ P(CH ₂) ₃ P(C ₆ H ₅) ₂)]BF ₄	525	26.5	190.2
10 [Rh(η^6 -C ₆ H ₅ CH ₃)(η^2 -(C ₆ H ₅) ₂ P(CH ₂) ₄ P(C ₆ H ₅) ₂)]BF ₄	585	42.1	198.0
11 ^c [Rh(η^6 : η^1 -PhO(CH ₂) ₂ PPh ₂)(η^1 -PhO(CH ₂) ₂ PPh ₂)]BF ₄	573	32.6, 34.9	198.7, 210.4
12 ^c [Rh(η^6 : η^1 -Ph(CH ₂) ₃ PPh ₂)(η^1 -Ph(CH ₂) ₃ PPh ₂)]BF ₄	515	36.6, 39.8	203.9, 198.8

^a Differential pulse voltammetry (DPV): 0.1 M ⁿBu₄NPF₆/CH₂Cl₂ at 21 °C vs FcH/FcH⁺. ^b CD₂Cl₂. ^c Reference 4a.

**Figure 1.** Graph of rhodium–phosphorus coupling constant versus number of methyl substituents for complexes **1–7**.

Each of the ³¹P NMR spectra for compounds **1–10** exhibits a single resonance with $J_{\text{Rh-P}}$ values of 190–207 Hz Table 2. The resonances for the dppe complexes (**1–7**) are in the range δ 77.5–79.3. The nonchelated complex **8** exhibits a resonance further upfield at δ 35.3, while the dppp complex **9** and the dppb complex **10** exhibit resonances at δ 26.5 and 42.1, respectively. Such chemical shift differences between the bidentate bis(phosphine) ligands, the monodentate phosphines, and the chelated phosphinoalkylarenes, in **11** and **12**, are a function of the absence or presence of chelation and the chelate ring size.¹¹ The ³¹P NMR chemical shift values for **1–7**, **9**, and **10** are comparable to those reported in the literature for Rh(I) complexes with the same chelating bis(phosphine) ligands.^{11,12}

Within the family of complexes of the general formula [Rh(η^2 -dppe)(η^6 -C₆H_{6-n}X_n)]BF₄ (X = CH₃, and n = 0–6), **1–7**, additional methyl substituents on the arene have a small, but measurable, effect on the ³¹P NMR chemical shifts and coupling constants. In general, increased electron-donating ability of the arenes corresponds to an increase in the coupling between Rh and P in a linear fashion (Figure 1 and Table 2). Furthermore, the ³¹P NMR chemical shifts values for **1–7** are also affected by the number of methyl substituents on the arene ring. Overall, increased electron richness of the arene leads to higher chemical shifts, although this effect trails off with increasing substitution on the arene. The electron richness of the arene ligand,

**Figure 2.** ORTEP drawing of **5**. Thermal ellipsoids are drawn at 30% probability. BF₄ group is omitted for clarity.

however, is not the only factor which contributes to the chemical shift and coupling constant values in the ³¹P NMR spectra of **1–7**.¹³ For example, slight structural changes within this family of compounds must also contribute to these spectroscopic values. For example, increased substituents on the arene most likely result in increased steric interactions between the methyl groups and the phenyl groups that are part of the bis(phosphine) ligands. This would be expected to influence the P–Rh–P bond angle and contribute to the trends observed in the ³¹P NMR spectra.

Solid-State Characterization of 5, 8, and 12. The structures of complexes **5**, **8**, and **12** were determined by single-crystal X-ray diffraction methods (Figures 2–4). Selected bond lengths and angles are given in Table 3. An ORTEP diagram of cation **5** is shown in Figure 2. The Rh atom sits in a bis(phosphine), η^6 -arene piano-stool geometry, and the P–Rh–P angle of 83.76° compares well with other complexes containing the Rh-dppe fragment (82.1–84.8°).¹⁴ The Rh–P bond lengths (Rh–P_{avg} = 2.219 Å) also compare well with the only example in the literature of a similar Rh bis(phosphine), η^6 -arene complex, [Rh(η^2 -dppe)(η^6 -C₆H₅BPh₃)] (P–Rh–P = 84.3°, Rh–P_{avg} = 2.221 Å).^{14c} The arene ring in complex **5** is not planar (average deviation = 0.0240 Å) but rather adopts a boat conformation with the bow and stern pointing toward the Rh center. Through theoretical calculations done by others, the origin of this

(13) It is well-known that electronic and structural factors dictate the chemical shifts and especially the coupling constants for such metal compounds. For more information, see: Verkade, J. G.; Quin, L. D. *Phosphorus-31 NMR Spectroscopy in Stereochemical Analysis*; VCH Publishers: Deerfield Beach, FL, 1987.

(14) (a) Becalski, A. G.; Cullen, W. R.; Fryzuk, M. D.; James, B. R.; Kang, G.-J.; Rettig, S. J. *Inorg. Chem.* **1991**, *30*, 5002. (b) Chan, A. S. C.; Shieh, H.-S.; Hill, J. R. *J. Organomet. Chem.* **1985**, *279*, 171. (c) Albano, P.; Aresta, M.; Manasero, M. *Inorg. Chem.* **1980**, *19*, 1069. (d) Chan, A. S. C.; Pluth, J. J.; Halpern, J. *Inorg. Chim. Acta* **1979**, *37*, L477. (e) Hall, M. C.; Kilbourn, B. T.; Taylor, K. A. *J. Chem. Soc., Dalton Trans.* **1970**, 2539.

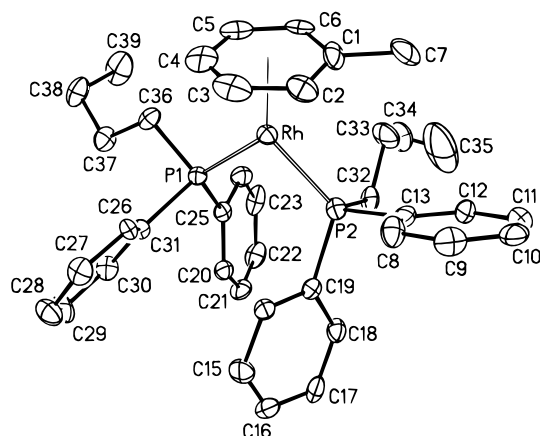
(10) (a) McFarlane, W.; Grim, S. O. *J. Organomet. Chem.* **1966**, *5*, 147. (b) Price, J. T.; Sorensen, T. S. *Can. J. Chem.* **1968**, *46*, 515. (c) Mann, B. E. *Chem. Commun.* **1971**, 976. (d) Köhler, F. H. *Chem. Ber.* **1974**, *107*, 570.

(11) Garrou, P. E. *Chem. Rev.* **1981**, *81*, 229.

(12) Fornika, R.; Görls, H.; Seemann, B.; Leitner, W. *J. Chem. Soc., Chem. Commun.* **1995**, 1479.

Table 3. Selected Distances (Å) and Angles (deg) for Complexes **5**, **8**, and **12**

complex 5		complex 8		complex 12	
Rh–P(1)	2.217(1)	Rh–P(1)	2.244(3)	Rh–P(1)	2.228(2)
Rh–P(2)	2.222(1)	Rh–P(2)	2.258(3)	Rh–P(2)	2.251(1)
Rh–C(1)	2.314(5)	Rh–C(1)	2.367(9)	Rh–C(1)	2.294(5)
Rh–C(2)	2.366(5)	Rh–C(2)	2.317(10)	Rh–C(2)	2.326(5)
Rh–C(3)	2.336(5)	Rh–C(3)	2.356(11)	Rh–C(3)	2.360(5)
Rh–C(4)	2.303(5)	Rh–C(4)	2.296(13)	Rh–C(4)	2.310(5)
Rh–C(5)	2.370(5)	Rh–C(5)	2.315(12)	Rh–C(5)	2.331(5)
Rh–C(6)	2.335(5)	Rh–C(6)	2.385(10)	Rh–C(6)	2.339(6)
Rh–arene cent.	1.87	Rh–arene cent.	1.88	Rh–arene cent.	1.84
P(1)–Rh–P(2)	83.76(4)	P(1)–Rh–P(2)	93.35(10)	P(1)–Rh–P(2)	91.44(6)

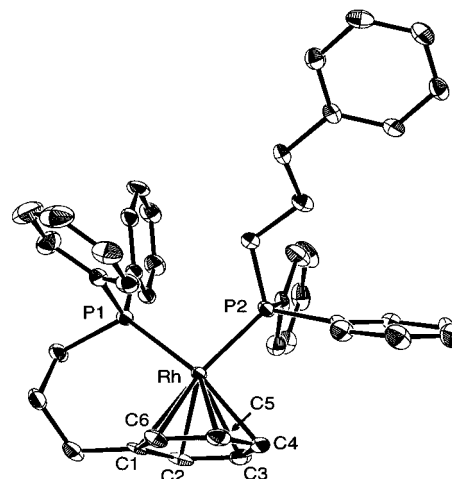
**Figure 3.** ORTEP drawing of **8**. Thermal ellipsoids are drawn at 30% probability. BF_4 group is omitted for clarity.

deformation is proposed to be of an electronic, rather than a steric, origin.¹⁵

An ORTEP diagram of complex **8** is shown in Figure 3. The Rh–P bond distances ($\text{Rh–P}_{\text{avg}} = 2.251 \text{ \AA}$) for complex **8** are longer than the average Rh–P distances for the other structurally characterized compounds reported herein. In addition, the Rh–arene centroid distance (1.88 Å) for this compound is longer than those for the other three structures (1.84–1.87 Å) and the P–Rh–P angle in **8** (93.35°) is larger than the P–Rh–P angle for the other three complexes ($91.75\text{--}83.75^\circ$). Presumably, these differences are, in part, a result of the bulky *n*-butyl diphenylphosphine ligands in **8**. The Rh–C bond distances follow a similar trend as the Rh–C bond distances in complex **5**. The arene ring in **8** is not planar, however, the boat conformation is less evident in this structure (average deviation = 0.0207 Å).

An ORTEP diagram of compound **12** is shown in Figure 4. In this complex, the two Rh–P bond distances are significantly different from each other. The Rh–P_{chelated} bond distance is 0.02 Å shorter than the Rh–P_{monodentate} bond distance. The P–Rh–P bond angle (91.44°) is very similar to that in **9** (91.74°). The η^6 -arene ring in complex **12** adopts a boat conformation with respect to Rh which is similar to complexes **5** and **8** (average deviation = 0.0169 Å). The structure of complex **12** is strikingly similar to the structure of complex **11**, which was described in a previous report, (Chart 1).^{4a,b} The Rh–P_{avg} and Rh–C_{avg} distances are virtually identical (**11**: Rh–P_{avg} = 2.24 Å, Rh–C_{avg} = 2.31 Å; **12**: Rh–P_{avg} = 2.24 Å, Rh–C_{avg} = 2.33 Å).

Electrochemical Studies. The oxidative electrochemistry of compounds **1–10** was studied by cyclic voltammetry (CV) and differential pulse voltammetry (DPV). CV and DPV of

**Figure 4.** ORTEP drawing of **12**. Thermal ellipsoids are drawn at 50% probability. BF_4 group is omitted for clarity.

compounds **1–10** were performed in CH_2Cl_2 at 21 °C with a 0.1 M solution of *n*- Bu_4NPF_6 as the supporting electrolyte, and all $E_{1/2}$ values are given versus the $\text{FcH}/[\text{FcH}]^+$ [$\text{Fc} = (\eta^5\text{-C}_5\text{H}_5)\text{-Fe}(\eta^5\text{-C}_5\text{H}_4)$] redox couple (Table 2). The redox couples for **4** and **6** have been confirmed to be one-electron-transfer processes via cyclic and rotating disk voltammetry experiments. On the basis of these studies, the reversible electrochemistry observed for **2, 3, 5, 7–10**, and **12** is also assumed to be associated with a Rh(I)/Rh(II) couple.

In order to study how the electronic character of the arene ligand affects the kinetic stability of the Rh(II) form of these bis(phosphine), η^6 -arene complexes, the electrochemical reversibility of the Rh(I)/Rh(II) redox couples for **1–7**, all of which contain the dppe ligand, was examined. The electrochemical behavior of the benzene complex, **1**, was irreversible at all scan rates measured (up to 1 V/s); presumably the decomposition of the Rh(II) form was due to loss of the weakly bound arene ligand. It is known that arene complexes of Rh(I) are extremely labile, and even though the strength of the Rh–arene interactions are expected to increase on going from Rh(I) to Rh(II), the susceptibility of the Rh center to ligand substitution reactions may also be greater for the Rh(II) form. Indeed, odd-electron compounds, such as the 17-electron Rh(II) oxidation product, often have substitutionally labile ligands.¹⁶ For example, in the case of the bulk electrolysis of an η^6 -arene, tricarbonyl chromium complex, 2-(2,3,4,5,6-pentamethylphenyl)ethanol]chromium tricarbonyl, a stoichiometric amount of the arene ligand is lost through a series of steps which start with the oxidation of the metal center from Cr(0) to Cr(I).^{16c} In

(15) (a) Muetterties, E. L.; Bleeke, J. R.; Wucherer, E. J.; Albright, T. A. *Chem. Rev.* **1982**, 82, 499. (b) Radovich, L. J.; Koch, F. J.; Albright, T. A. *Inorg. Chem.* **1980**, 19, 3373. (c) Albright, T. A.; Hoffmann, R.; Tse, Y.; D'Ottavio, T. *J. Am. Chem. Soc.* **1979**, 101, 3812.

(16) (a) Howell, J. A. S.; Burkinshaw, P. M. *Chem. Rev.* **1983**, 83, 557. (b) Albers, M. O.; Coville, N. J. *Coord. Chem. Rev.* **1984**, 53, 227. (c) Doxsee, K. M.; Grubbs, R. H.; Anson, F. C. *J. Am. Chem. Soc.* **1984**, 106, 7819. (d) Hershberger, J. W.; Klinger, R. J.; Kochi, J. K. *J. Am. Chem. Soc.* **1983**, 105, 61.

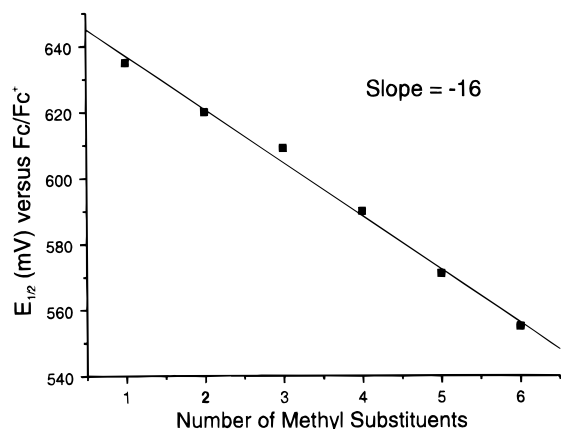


Figure 5. Graph of $E_{1/2}$ versus number of methyl substituents for complexes 2–7.

moving to methyl substituted arenes, complexes 2 and 3 exhibit reversible redox waves only at scan rates faster than 200 and 20 mV/s, respectively. In addition, those complexes with even more electron donating arene ligands (4–7) exhibit markedly increased kinetic stabilities for their Rh(II) forms as evidenced by the reversibility of their Rh(I)/Rh(II) redox couple at all measured scan rates. This is presumably due to the ability of the more electron donating arene ligands to coordinate more strongly to the Rh(II) centers generated by oxidation. Furthermore, increased alkyl substitution on η^6 -arene ligands has been proposed by others to protect metal centers from external attack through the increased steric bulk of the ligand.^{16c}

The $E_{1/2}$ values for 2–7, which are a measure of the thermodynamic stabilities of the Rh(II) forms, also follow a similar trend as the observed trend in kinetic stability. The half-wave potentials of these complexes decrease in a linear fashion by 16 mV with the addition of each methyl group (Figure 5). This reflects an increase in the electron richness of the Rh center upon the addition of each methyl substituent to the arene ligand. In a complementary study, Geiger and co-workers have observed similar, but larger shifts per added methyl groups (~ 26 mV), for the reduction potentials of Rh(III) cyclopentadienyl, η^6 -arene complexes.^{3c} Such shifts in half-wave potentials caused by the substitution of a hydrogen by an alkyl group at a π -ligand of a transition metal complex are commonly observed.¹⁷ However, it appears that the relative magnitude of the substituent effects for certain classes of compounds is dependent on how strongly the ligands with alkyl substituents coordinate to the metal centers of interest. For example, the arenes in the compounds studied by Geiger coordinate more strongly to the Rh(III) center than the arenes in this study bond to Rh(I), as evidenced by their ligand substitution behavior.^{3c} Similarly, the cyclopentadienyl groups of ferrocene bond significantly more strongly to Fe(II) than the arene ligands in this study bond to Rh(I). Accordingly, an approximately -50 mV change in $E_{1/2}$ values is observed with the addition of each methyl group to the cyclopentadienyl ligands in ferrocene.^{17a,b}

From the $E_{1/2}$ data presented in Table 2, correlations between the binding strength of the arene ligands and the stability of the Rh(II) forms of these complexes can be established. By comparing the arene substitution processes involving the Rh(I)

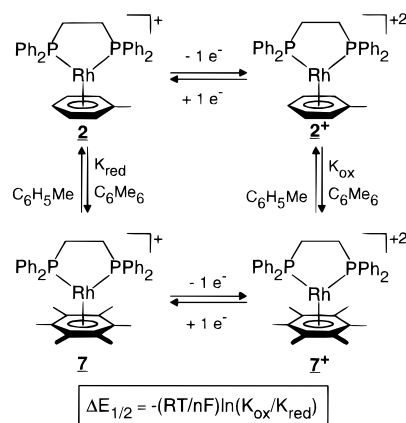
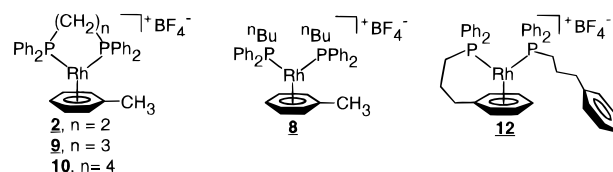


Figure 6. Square-wave diagram depicting the equilibria between 2 and 7 and 2⁺ and 7⁺.

Table 4. Ratio of K_{ox}/K_{red} for Rh(I)/Rh(II) Couple

complex	3	4	5	6	7
2	1.80	2.76	5.81	12.2	22.8
3	—	1.54	3.23	6.78	12.7
4	—	—	2.10	4.41	8.24
5	—	—	—	2.10	3.92
6	—	—	—	—	1.87

Chart 3



and Rh(II) forms of these complexes, as in the square wave diagram in Figure 6, a Nernstian relationship allows for calculation of the ratio of the ligand substitution equilibrium constants from $E_{1/2}$ values.¹⁸ In Figure 6, the equilibrium constant for the reaction of the Rh(II) form of 2 (2^+) with hexamethylbenzene (K_{ox}) is 22.8 times larger than the equilibrium constant for the reaction between the Rh(I) complex 2 and hexamethylbenzene (K_{red}). This is another way of showing that the Rh(II) form of 2 is significantly more stabilized than the Rh(I) species by electron-donating arene ligands such as hexamethylbenzene. Table 4 illustrates this relationship for complexes 2–7 and gives a quantitative measure of the extent of stabilization of the Rh(II) form as compared with that of the Rh(I) form for this family of compounds.

Complexes 2, 8–10, and 12 all possess tolyl-like ligands, yet their electrochemical behavior and $E_{1/2}$ values vary substantially (range = 130 mV) (Chart 3). In this case, the electrochemical responses for these bis(phosphine), monoalkylated η^6 -arene Rh(I) complexes may be due to the changes in the ligand connectivities and, hence, the different structures of each complex. By comparing the electrochemistry of these five complexes and considering the structural consequences on the electronic nature of the Rh center, the importance of two different types of chelation in the stabilization of Rh(II) in a piano-stool geometry can be assessed.

Upon examining the reversibility of the Rh(I)/Rh(II) redox couples, one can determine which ligands kinetically stabilize the Rh(II) form toward decomposition reactions. As stated earlier, compounds 11 and 12 exhibit reversible Rh(I)/Rh(II) redox couples at all scan rates measured (10 mV/s–1 V/s) (Figure 7).^{4a,b} In contrast, complexes 2 and 8 exhibit reversible

(17) (a) Koelle, U.; Khouzami, F. *Angew. Chem., Int. Ed. Eng.* **1980**, *8*, 640. (b) Robbins, J. L.; Edelstein, N.; Spencer, B.; Smart, J. C. *J. Am. Chem. Soc.* **1982**, *104*, 1882. (c) Koelle, U.; Fuss, B.; Rajasekharan, M. V.; Ramakrishna, B. L.; Ammeter, J. H.; Böhm, M. C. *J. Am. Chem. Soc.* **1984**, *106*, 4152. (d) Yur'eva, L. P.; Peregodova, S. M.; Nekrasov, L. N.; Korotkov, A. P.; Zaitseva, N. N.; Zakurin, N. V.; Vasil'kov, A. Y. *J. Organomet. Chem.* **1981**, *219*, 43. (e) Hamon, J.-R.; Astruc, D.; Michaud, P. *J. Am. Chem. Soc.* **1981**, *103*, 758.

(18) Evans, D. H. *Chem. Rev.* **1990**, *90*, 739.

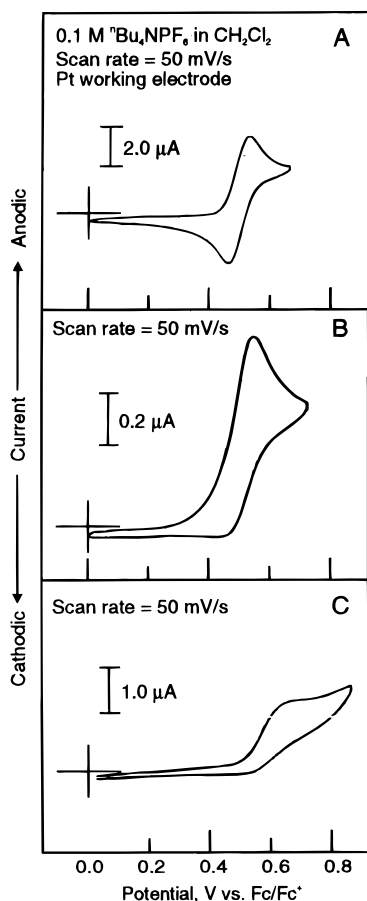


Figure 7. Cyclic voltammetry of (A) **12**, (B) **8**, and (C) **2**.

Rh(I)/Rh(II) redox couples only at scan rates greater than 200 mV/s (Figure 7). Upon the addition of a single methylene unit to the alkane bridge in **2**, the resulting dppp complex (**9**) exhibits reversible electrochemical behavior at all scan rates measured (10 mV/s–1 V/s). With the addition of one more methylene unit to the ligand backbone, the dppb complex **10** exhibits a reversible redox couple only when one scans faster than 20 mV/s. Thus, by cyclic voltammetry, only **9** and **12** exhibit chemically reversible waves at all scan rates measured (10 mV/s–1 V/s). From these observations, one can conclude that the ligand arrangements in **9** and **12** kinetically stabilize the Rh(II) form toward decomposition reactions. For **12**, this can be easily explained by the presence of the chelated η^6 -arene ligand. Apparently, the chelation in **12** kinetically stabilizes the Rh(II) form from decomposition by inhibiting dissociation of the arene ligand from the metal complex (in the cases of **2**, **8**, and **10** there is no arene chelation) and by sterically protecting the Rh(II) center from further reactions. The reason for compound **9**'s increased stability relative to **2**, **8**, and **10** is a bit more complex but can be rationally explained (vide infra).

In the literature, polydentate and bulky phosphine ligands have been used to stabilize mononuclear Rh(II) complexes, where, in addition to the usual chelate effect stabilization, the ligand backbone protects the periphery of the complex from external attack.^{3c,19} Surprisingly, for our complexes, a comparison of the redox potentials of **2**, **8–10**, and **12** reveals that the bidentate, chelated bis(phosphine) ligands in **2** and **10** thermodynamically destabilize the Rh(II) form of the complex relative to the other ligand arrangements (Table 2). The $E_{1/2}$

values of **2** (635 mV) and **10** (585 mV) are significantly higher than the $E_{1/2}$ values of **8** and **12** (505 and 515 mV, respectively), which do not contain bis(phosphine) chelation. In **10**, the longer alkane bridge between the two P atoms seems to enhance the stability of the oxidized complex as compared with complex **2**, which possesses an ethylene bridge. However, the oxidized forms of both **2** and **10** are less thermodynamically favored in comparison with the oxidized form of **9** (525 mV), which has a propylene bridge. Within the chelating bis(phosphine) complexes (**2**, **9**, and **10**) complex **9** seems to be an exception. With an $E_{1/2}$ value only slightly higher than those measured for **8** and **12**, it is the most easily oxidized complex out of all the bis(phosphine) chelates presented herein (**1–7**, **10**). Its Rh(II) form, however, is slightly less favored than those of compounds **8** and **12**. Those complexes without bis(phosphine) chelation, such as **8** and **12**, are the easiest to oxidize and, therefore, their Rh(II) forms are the most thermodynamically stable.

From our comparison of the chemical reversibilities and half-wave potentials of the Rh(I)/Rh(II) redox couples for compounds **2**, **8–10**, and **12**, we can identify several of the important factors which contribute to the electronic nature of the Rh center and stability of Rh(II) oxidation state in the different ligand environments. We have found that the most favorable environment for Rh(II) with piano stool geometry among the complexes **2**, **8–10**, and **12** is defined by the (phosphinoalkyl)arene ligands in **12**. In this complex, not only is the Rh center one of the most electron rich of the series ($E_{1/2} = 515$ mV), but it is also the most kinetically stable Rh(II) form as evidenced by its reversible behavior at all measured scan rates. Complex **8**, in comparison, oxidizes at a slightly lower potential ($E_{1/2} = 505$ mV) but exhibits irreversible behavior at scan rates less than 200 mV/s. In addition, complex **9** is reversible at all scans rates; however, it oxidizes at a slightly higher potential than **8** and **12**, and therefore, its Rh(II) form is not as thermodynamically favored.

Structural and Electrochemical Correlation of 2, 8–10, and 12 Using EHMO Calculations. As stated earlier, complexes **8**, **9**, and **12** oxidize at significantly lower potentials than those of complexes **2** and **10**. Unlike the trend observed for complexes **1–7**, a correlation between the different ligand connectivities and the relative stabilities of the corresponding Rh(II) forms is not evident when one only considers the structural characteristics of these compounds in their reduced state and the corresponding electrochemical data. For example, one might expect those complexes with the longest Rh–P bonds to be the least electron rich and, therefore, the most difficult to oxidize, especially if σ -donation from the phosphine ligands is the dominant factor which controls the electron richness of the Rh center. Alternatively, if Rh-to-P back-bonding is the dominant factor that dictates the Rh electron-rich character in this series of complexes, the compounds with the longest Rh–P bonds should be the easiest to oxidize. However, if one examines the structural data, there is no correlation between the Rh–P bond lengths and the $E_{1/2}$ values for this series of compounds. By also taking into account the structures of the oxidized forms of complexes **2**, **8–10**, and **12** and theoretical data, the experimentally defined trend in $E_{1/2}$ values can be rationally explained.

Although, thus far we have not isolated the Rh(II) forms of these complexes, Harlow et al. have studied an isoelectronic and isostructural cobalt system. For example, their work shows that significant structural changes occur after oxidation of a bis-(triethylphosphine)cyclopentadienylcobalt(I) complex.²⁰ Upon oxidation of the Co(I) center to Co(II), the complex undergoes substantial changes in both its Co–P bond distances (2.218–

(19) (a) Haefler, S. C.; Dunbar, K. R.; Bender, C. *J. Am. Chem. Soc.* **1991**, *113*, 9540. (b) Bianchini, C.; Laschi, F.; Ottaviani, M. F.; Peruzzini, M.; Zanello, P.; Zanobini, F. *Organometallics* **1989**, *8*, 893. (c) Masters, C.; Shaw, B. L. *J. Chem. Soc. (A)* **1971**, 3679.

2.230 Å) and the P–Co–P bond angle (98.49–101.2°), while the Co–Cp distances remain essentially unchanged (2.084–2.083 Å). The origin of the observed structural perturbations was easily understood upon careful consideration of the nature of the highest occupied molecular orbital (HOMO) and its role in the small amount of metal to phosphine ligand π -back-bonding present in the complex. From extended Hückel calculations, the metal d orbital component of the HOMO was determined to be orthogonal to both the Co–P bonds and, thus, a π -interaction between this orbital and an empty phosphorus p and/or d orbital was symmetry allowed. This π -back-bonding interaction was used to explain the counterintuitive lengthening of the Co–P bonds and widening of the P–Co–P angle. For instance, removal of an electron from the metal d orbital decreases the amount of π -back-bonding, thereby weakening and lengthening the Co–P bonds. The enlargement of the P–Co–P angle also reflects the decrease in the π -interactions, which have optimum overlap at a smaller and more sterically congested angle. On removing an electron from the HOMO, the π -back-bonding is weakened and the P–Co–P angle opens up to relieve the unfavorable steric interactions present.

Although the work of Harlow et al. studies the changes in structure upon metal complex oxidation, the consequences of chelation in such structures with regard to their electrochemical behavior was not addressed. If the HOMOs of the complexes studied herein are similar in nature to those studied by Harlow et al., then one would expect complexes **2**, **8–10**, and **12** to undergo a similar widening of the P–Rh–P angle and lengthening of the Rh–P bonds upon oxidation of the metal center from Rh(I) to Rh(II). Thus, complexes that are more constrained in their P–Rh–P bond angle would be less able to accommodate this electrochemically induced structural change and, in general, would oxidize at higher potentials. In order to identify the HOMOs in these complexes, theoretical investigations of complexes **2**, **8–10**, and **12** using extended Hückel molecular orbital (EHMO)²¹ calculations were performed. The HOMOs and LUMOs for **5**, **8**, **9**, and **12** were calculated using crystallographic coordinates for each complex; the MOs of compound **5** were used as a model for those of **2** even though the arene ligand is different, since the P–Rh–P angle for mononuclear dppe compounds of Rh(I) fall within a relatively narrow range (82.1–84.8°)¹⁴ and the Rh–arene bond distances for all the structurally characterized compounds are very similar.

Other workers have studied the nature of the molecular orbitals of similar piano stool complexes.¹⁵ For example, Muetterties et al. have calculated the molecular orbitals for M(arene)L₂ piano-stool complexes.^{15a} Using the crystallographic coordinates, the MOs calculated for our compounds are similar to those in the general model presented by Muetterties and, more importantly, the HOMOs for these complexes are similar to those reported for the bis(triethylphosphine)cyclopentadienylcobalt(I) complex.²⁰ In Figure 8, the HOMO of complex **8** is shown and is representative of the calculated HOMOs for all the structurally characterized complexes. In the calculated HOMO, the major component is the metal d orbital, and although the π -interaction is too small to show up in the orbital plot, an examination of the wave function reveals that such bonding contributions involving phosphorus p and d orbitals do exist. From these calculations, one can see that the structural changes upon oxidation, due to weakening the Rh-to-P π -back-bonding interactions, are also likely for the

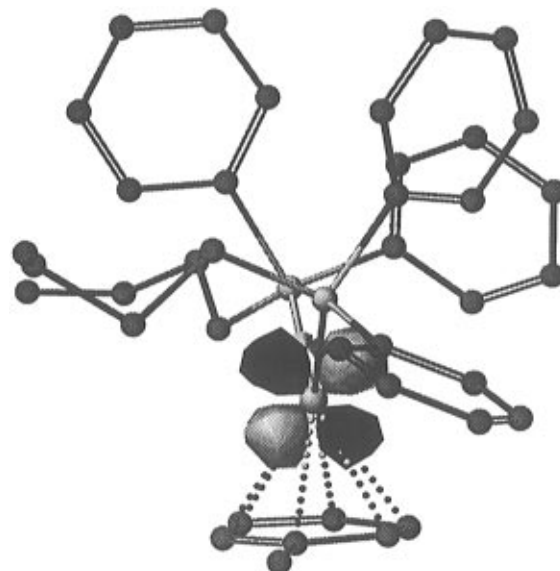


Figure 8. HOMO of **8** obtained from an EHMO calculation using the crystallographic coordinates. This is a representative of the HOMO for complexes **2**, **8–10**, and **12**.

piano-stool complexes in this study. If this is the case, then those ligands which are most able to accommodate the widening of the P–Rh–P angle and the lengthening of the Rh–P bonds will be the easiest to oxidize. Indeed, from the electrochemical data, it is the more strained bis(phosphine) chelated complexes (**2** and **10**) which give the highest half-wave potentials. In addition, it is the exception (compound **9**) which possesses the bis(phosphine) alkyl bridge that has the least amount of ring strain and is the easiest to oxidize out of the bis(phosphine) chelates.²² Moreover, it is the complexes which are not restricted in their P–Rh–P bond angle by bis(phosphine) chelation which have the two lowest $E_{1/2}$ values. In particular, it is the formation of the Rh(II) species which contains no chelation at all (**8**) which is the most thermodynamically favored of the whole series. Presumably, the structural constraints in this complex are the least, and it can easily accommodate the changes induced by the oxidation of the metal center.

Conclusions

The systematic studies presented herein show that: (1) more electron-rich arene ligands kinetically stabilize the Rh(II) forms of these complexes and thermodynamically stabilize the Rh(II) forms of these complexes by 16 mV per methyl group; (2) chelation of the (phosphinoalkyl)arene ligand offers kinetic stability to Rh(II) piano-stool complexes from loss of arene ligand upon oxidation relative to the complexes without arene chelation; (3) bidentate chelation of the bis(phosphine) ligand with an ethyl and butyl bridge thermodynamically destabilizes the Rh(II) forms of these complexes; and (4) those complexes which contain the least constrained P–Rh–P angle most favor the formation of Rh(II). In addition, although the trends in the properties of the reduced form of many complexes usually parallels their oxidative electrochemical trends, we have shown that this is not always the case. Moreover, it is necessary to consider what happens to the structure of a complex upon going from one oxidation state to another in order to understand the observed electrochemical data. Indeed, we predict that other systems, which employ restricted chelating ligands and undergo

(20) Harlow, R. L.; McKinney, R. J.; Whitney, J. F. *Organometallics* **1983**, *2*, 1839.

(21) CAChe extended Hückel program, CAChe Scientific, Beaverton, OR.

(22) Li, C.; Cucullu, M. E.; McIntyre, R. M.; Stevens, E. D.; Nolan, S. P. *Organometallics* **1994**, *13*, 3621.

structural changes involving those ligands upon electrochemical oxidation or reduction will experience a similar energetic penalty as the system described herein. Finally, from the results in this study, a logical strategy to prepare isolable Rh(II) compounds with piano-stool geometry is to prepare chelating (phosphino-alkyl)arene ligands with strongly donating arene substituents; this is a strategy we are currently pursuing.

Acknowledgment. We acknowledge the NSF (CHE-9625391) and (CHE-9357099), and the Petroleum Research Fund (No. 30759-AC3) for generously funding this research.

We are also grateful to Professor Guy Orpen for directing us toward the work of Harlow et al.

Supporting Information Available: Detailed descriptions of the X-ray diffraction studies for **5**, **8**, **9**, and **12**, including tables of experimental details, atom positional parameters, equivalent isotropic displacement parameters, bond lengths, bond angles, anisotropic displacement parameters, and mean plane calculations (39 pages). See any current masthead page for ordering and Internet access instructions.

JA963384V